Available online at www.sciencedirect.com
SCIENCE DIRECT®
Carbohydrate Research 340 (2005) 2171–2184
Carbohydrate RESEARCH

On the generalized valence bond description of the anomeric and exo-anomeric effects: an ab initio conformational study of 2-methoxytetrahydropyran

Rodrigo S. Bitzer,[a] André G. H. Barbosa,[b] Clarissa O. da Silva[c,*] and Marco A. C. Nascimento[a]

[a]*Departamento de Físico-Química, Instituto de Química, Universidade Federal do Rio de Janeiro, Rio de Janeiro, RJ 21949-900, Brazil*
[b]*Departamento de Química Orgânica, Instituto de Química, Universidade Federal Fluminense, Niterói, RJ 24210-150, Brazil*
[c]*Departamento de Química, Instituto de Ciências Exatas, Universidade Federal Rural do Rio de Janeiro, Seropédica, RJ 21890-000, Brazil*

Received 19 April 2005; received in revised form 22 June 2005; accepted 6 July 2005
Available online 28 July 2005

Abstract—An ab initio conformational study of the α- and β-glycosidic C1–O1 bonds has been carried out on the axial and equatorial forms of 2-methoxytetrahydropyran (2-MTHP) at the HF/6-31G(d,p) and GVB-PP/6-31G(d,p) levels of calculation. Six conformers of 2-MTHP were fully optimized at both levels. The calculations have shown that the conformer containing the (+sc) orientation around the axial C1–O1 bond is the most stable one and is favored over that bearing the (−sc) arrangement about the equatorial C1–O1 bond by 1.39 (HF) and 1.52 (GVB-PP) kcal/mol. The potential energy surfaces for rotating about the axial and equatorial C1–O1 bonds were constructed at the HF and GVB-PP levels. For each form of 2-MTHP the HF and GVB-PP potential curves exhibit similar profiles. This shows that both methods provide similar descriptions for the position of the conformational minima and for the values and location of the rotational barriers. In addition to the conformational study, a discussion concerning the nature of the chemical bond in acetal fragments and the origin of the anomeric and exo-anomeric effects is presented in terms of optimized non-orthogonal GVB orbitals of 2-MTHP. The intramolecular factors that respond for the order of stability and conformational changes in bond lengths of the conformers of 2-MTHP are examined in light of the GVB description. The problems associated with the use of the NBOs (natural bond orbitals) to analyze chemical bonding in the acetal fragments are discussed, and the choice for the GVB-PP description is justified.

Keywords: Ab initio; Localized wave function; 2-Methoxytetrahydropyran; Glycosidic bond; Anomeric effect

1. Introduction

Carbohydrates play a central role in a number of biochemical processes.[1] Their biological functions are strictly related to their three-dimensional structures, which are to a greater extent defined by the conformational preference about each glycosidic C1–O1–Ci linkage.[2,3] Therefore, a conformational study of the α- and β-glycosidic C1–O1 bonds is of utmost relevance to a proper understanding of the relationship between activity, reactivity, and chemical structure of oligo- and polysaccharides.

Inter-[4] and intramolecular[5–12] effects dictate the conformational behavior of acetal C5–O5–C1–O1–Ci fragments in carbohydrates. From the intramolecular point of view, the anomeric[5–10] and exo-anomeric[5,10–12] effects are the most important ones in predicting, respectively, the rotational preference of the endocyclic O5–C1 bond and that of the exocyclic C1–O1 bond. The anomeric effect refers to the unexpected thermodynamic preference for the axial position of a more electronegative substituent, such as methoxyl or chloride, bound

* Corresponding author. Tel./fax: +55 21 2682 2807; e-mail: clarissa-dq@ufrrj.br

0008-6215/$ - see front matter © 2005 Elsevier Ltd. All rights reserved.
doi:10.1016/j.carres.2005.07.001

to the anomeric carbon atom (C1). In turn, the exo-anomeric effect relates to the preference for the (+sc) or (−sc) (sc = synclinal or gauche) arrangements about the α- and β-glycosidic C1–O1 bonds. Although the anomeric and exo-anomeric effects have been widely discussed in carbohydrate chemistry, they may be also recognized in simpler cyclic or acyclic molecules containing the acetal C–O–C–O–C fragment.[5,9–12] Thus, one can build model compounds with such a fragment to investigate the anomeric and exo-anomeric effects using high-level quantum-chemical methodologies.[5,13–25]

To computationally study the conformational behavior of acetal fragments in methyl-α- and β-D-pyranosides, we have chosen the axial and equatorial forms of 2-methoxytetrahydropyran (2-MTHP) as prototype compounds. Figure 1 illustrates the axial and equatorial conformers of 2-MTHP that are relevant to the present study. The conformational analysis of 2-MTHP primarily involves a scanning on two dihedral angles, namely θ [C5–O5–C1–O1] and ϕ [O5–C1–O1–Ci].[5] The values expected for these two torsion angles are given in Figure 1. The notation used to identify the conformers of 2-MTHP (Fig. 1) is similar to that proposed elsewhere.[5]

2-MTHP is one of the smallest cyclic molecules bearing the acetal C–O–C–O–C moiety, which is also present in all oligo- and polysaccharides. For this reason, many semiempirical,[26–28] molecular mechanics,[16,29–34] ab initio molecular orbital (MO),[4,14–17,20] and density functional theory (DFT)[19,20,33] calculations have been performed to study the conformational behavior of 2-MTHP. Among the ab initio MO calculations, the work by Tvaroška and Carver[16] is one of the most complete in the literature. In that paper,[16] the geometries of the six conformers of 2-MTHP were optimized at HF/4-21G and 6-31G(d), and MP2/6-31G(d) levels. Regardless of the level of calculation, Tvaroška and Carver verified the following order of growing stability: (+sc, −sc) < (ap, ap) < (ap, +sc) < (+sc, ap) < (ap, −sc) < (+sc, +sc). Moreover, those authors showed that the axial (+sc, +sc) conformer is favored over the equatorial (ap, −sc) one by 3.67 (HF/4-21G), 1.47 (HF/6-31G(d)), and 2.23 (MP2/6-31G(d)) kcal/mol. Other ab initio MO studies, however, were concerned solely with the optimization of just a few conformers of 2-MTHP.[14,15,17] For instance, Wiberg and Murcko[14] verified that the (+sc, +sc) conformer is 1.33 kcal/mol more stable than the (ap, −sc) one at the HF/6-31G(d)//3-21G level. Experimental data on the axial-equatorial equilibrium of 2-MTHP and of its methylated derivatives have also revealed the preference for the axial forms.[11,12,35–41] de Hoog et al.[12] pointed out, from NMR and dipole moment measurements that only two (or three) conformers of 2-MTHP might occur in

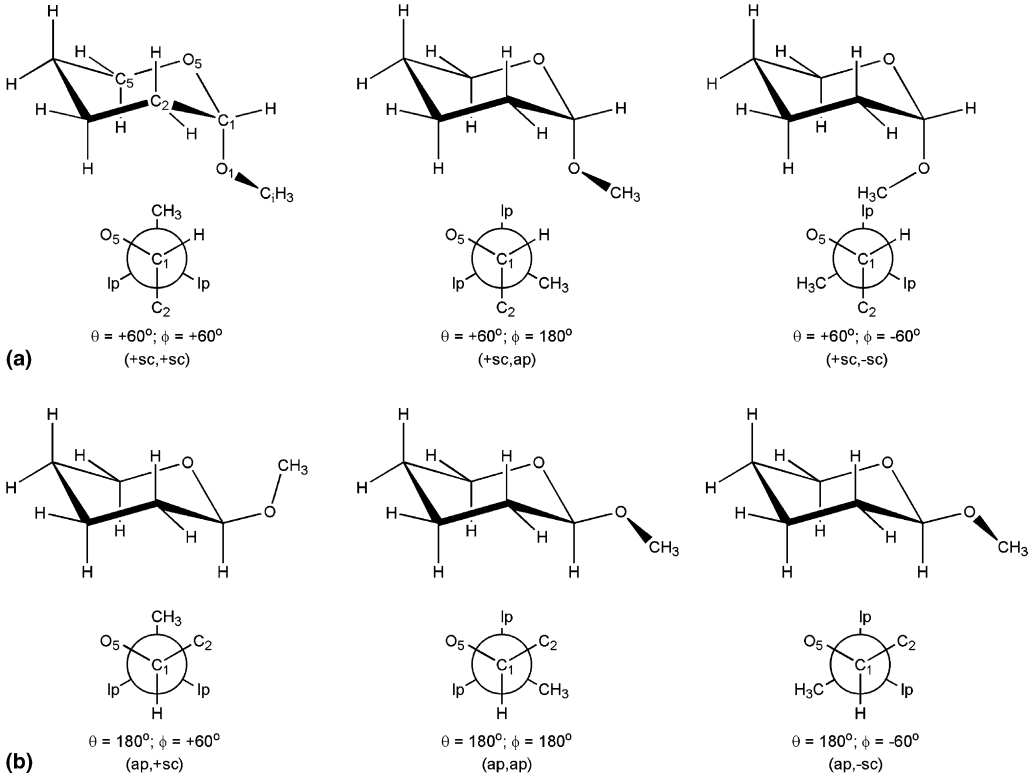

Figure 1. Axial (a) and equatorial (b) conformers of 2-methoxytetrahydropyran and their Newman's projections along the exocyclic C1–O1 bond (lp stands for lone pair). The notation in parentheses indicates the orientation expected for the dihedral angles θ and ϕ, respectively. (sc) and (ap) stands for synclinal (or gauche) and antiperiplanar (or trans), respectively.

non-polar solutions: one axial (the most stable one) and one (or two) equatorial conformers. More recently, Wiberg and Marquez[38] verified that in the gas phase the difference in enthalpy between the equatorial and axial forms of 4,6-dimethyl-2-methoxytetrahydropyran (4,6-Me_2-2-MTHP) is of 1.21 ± 0.07 kcal/mol in favor of the latter.

The origin of the anomeric and exo-anomeric effects is mainly attributed to the $n_{O5} \rightarrow \sigma^*_{C1-O1}$ and $n_{O1} \rightarrow \sigma^*_{C1-O5}$ electronic hyperconjugation effects, respectively,[5,14–17,20] and the natural bond orbital (NBO) analyses[15,17,20] based on the results of ab initio MO calculations on 2-MTHP have been used in support of this belief. These hyperconjugative interactions are assumed to have some geometric consequences.[5,14–17,20] In general, Hartree–Fock (HF) studies of 2-MTHP have shown that in the axial conformers the O5–C1 bond lengths are slightly shorter than those obtained for the equatorial ones.[14–16] This behavior has been interpreted as a result of the $n_{O5} \rightarrow \sigma^*_{C1-O1}$ interaction, which is assumed to be favored only in the axial structures. Furthermore, preference for the (+sc) or (−sc) arrangements about the axial and equatorial C1–O1 bonds is often accompanied by a decrease in the C1–O1 bond distances in relation to the O5–C1 bond distances.[14–17] Such structural trends have been ascribed to the $n_{O1} \rightarrow \sigma^*_{C1-O5}$ hyperconjugative effect. In fact, the geometric trends theoretically discussed for the conformers of 2-MTHP have been reproduced in a large number of crystal structures of methyl-α- and β-D-pyranosides and oligosaccharides.[2,5,13] For this reason, the use of the electronic hyperconjugation concept to explain the origin of the anomeric and exo-anomeric effects has been widely accepted.

An ab initio conformational analysis of the α- and β-glycosidic C1–O1 bonds using valence bond (VB)-type wave functions has never been carried out. Thus, in this paper we investigate if a localized description, which does not include any couplings between oxygen lone pairs and σ* orbitals, can account for the conformational energies and geometric trends of the axial and equatorial conformers of 2-MTHP. Therefore, the present work focuses on the use of the generalized valence bond-perfect pairing (GVB-PP) wave function[42] to describe the electronic structure of the six conformers of 2-MTHP. We present the results of a full geometry optimization of these conformers at the GVB-PP level and a comparison between these results and those obtained at the HF level, using the same basis set [6-31G(d,p)]. In addition, from the analysis of optimized atomic-centered non-orthogonal singly occupied GVB orbitals of 2-MTHP, we examine the nature of the chemical bonds in axial and equatorial acetal fragments and the origin of the anomeric and exo-anomeric effects.

2. Computational details

All calculations were carried out in vacuum at the HF/6-31G(d,p) and GVB-PP/6-31G(d,p) levels of calculation, using the Jaguar 3.5 program[43] with an energy convergence criterion of 5.00×10^{-8} hartrees. The initial guess geometries were first obtained from the corresponding centers of methyl-α- and β-D-glucose, whose structures were optimized using the Dreiding II force field.[44] Second, from the axial or equatorial geometry derived for 2-MTHP, the value of the dihedral angle ϕ was chosen so as to correspond to that expected for each conformer (Fig. 1). This procedure provided six initial guess geometries for 2-MTHP. The starting structures of the (+sc, +sc), (+sc, ap), (+sc, −sc), (ap, +sc), and (ap, −sc) conformers were fully optimized at both HF and GVB-PP levels. As will be discussed in Section 3.1, the geometry optimization of the (ap, ap) conformer was only achieved after freezing ϕ at 210.00° in both HF and GVB-PP calculations. The vibrational frequencies of the optimized HF and GVB-PP geometries were calculated and verified to be real. This showed that these structures correspond to conformational minima in the potential energy surface of 2-MTHP.

To construct the potential curves for rotation about the axial and equatorial C1–O1 bonds of 2-MTHP, we performed a scan on ϕ using an interval of 10° at the HF/6-31G(d,p) level. At the GVB-PP/6-31G(d,p) level, however, an interval of 30° was employed. The HF and GVB-PP potential curves were generated by a fitting procedure using five-term Fourier-type expansions, whose analytical expressions will be reported in detail in a forthcoming publication.

For the GVB-PP calculations, all valence electrons were correlated, comprising 24 GVB pairs for each conformer, 20 of them corresponding to the bonds and the other 4 to the oxygen lone pairs [GVB-PP(24/48)]. In the perfect pairing (PP) approach,[42] each GVB pair is built from two atomic-centered non-orthogonal singly occupied orbitals. In the computational implementation of the GVB-PP method, core orbitals are treated as HF orbitals, and each pair of singlet-coupled non-orthogonal GVB orbitals is transformed into a corresponding pair of orthogonal orbitals, called the first and the second GVB natural orbitals.[42] At the end of each GVB-PP geometry optimization, each optimum GVB pair of natural orbitals can be always converted into its corresponding pair of non-orthogonal GVB orbitals by a simple linear transformation. These non-orthogonal GVB orbitals of 2-MTHP are used in the discussion about the nature of the chemical bond in acetal moieties and about the origin of the anomeric and exo-anomeric effects (Section 3.3).

3. Results and discussion

3.1. Conformational energies

The values of the dihedral angles ϕ and the total relative energies (ΔE_T) calculated for the conformational minima of 2-MTHP, at the HF/6-31G(d,p) and GVB-PP/6-31G(d,p) levels, are provided in Table 1. These data show that the axial (+sc, +sc) conformer is the most stable one at both HF and GVB-PP levels. The second most stable conformer is the equatorial (ap, −sc) one. At the GVB-PP/6-31G(d,p) level, the total energy difference between the (ap, −sc) and (+sc, +sc) conformers is of 1.52 kcal/mol, that is, 0.13 kcal/mol higher than the value calculated at the HF/6-31G(d,p) level. The results in Table 1 show that the GVB-PP relative energies are all slightly higher than those obtained at the HF level. The thermodynamic preference for the axial (+sc, +sc) conformation agrees with previous ab initio studies on 2-MTHP[14–17] and with the gas-phase experimental result for 4,6-Me_2-2-MTHP.[38] The order of stability described in Table 1 is similar to that reported by Tvaroška and Carver.[16]

Table 1. Orientation (ϕ, deg) and relative energies (ΔE_T, kcal/mol) of the conformational minima of 2-methoxytetrahydropyran calculated at the HF/6-31G(d,p) and GVB-PP/6-31G(d,p) levels

Conformer	HF/6-31G(d,p)[a]		GVB-PP/6-31G(d,p)[b]	
	ϕ	ΔE_T	ϕ	ΔE_T
(+sc, +sc)	64.59	0.00	64.10	0.00
(ap, −sc)	−63.08	1.39	−62.89	1.52
(+sc, +ac)[c]	140.92	3.93	141.24	3.95
(ap, +sc)	54.75	4.31	54.64	4.36
(ap, ap)[d]	210.00	5.95	210.00	5.98
(+sc, −sc)	−47.46	10.46	−47.15	10.55

[a] The absolute total energy for the (+sc, +sc) structure is −383.928428 hartrees.
[b] The absolute total energy for the (+sc, +sc) structure is −384.291191 hartrees.
[c] The proper designation of this conformer is (+sc, +ac), instead of (+sc, ap), because the optimum values of ϕ correspond to the +anticlinal (+ac) orientation.
[d] Conformer obtained at a fixed angle of 210.00°.

The HF and the GVB-PP methods provide quite different pictures of the molecules. In the former approach, a molecule is described in terms of molecular orbitals, which are, in general, delocalized over the entire molecule. In the GVB-PP approach, however, the identity of the atoms is greatly preserved, and the molecule is viewed as a collection of atoms held together by chemical bonds, these ones resulting from the singlet coupling between adjacent atomic-localized non-orthogonal singly occupied orbitals. In spite of the differences, it is interesting to observe that both HF and GVB-PP calculations on 2-MTHP provide the same order of stability for its conformers (Table 1).

Even though the ab initio MO calculations on 2-MTHP have indicated the (+sc, +sc) conformer as the most stable one,[14–17,20] the values of the relative energies of the conformers (ΔE_T) are somewhat sensitive to the ab initio method and basis set used, as shown in Table 2. At the HF/3-21G level,[14] the total energy difference between the two most stable conformers of 2-MTHP is more than twice as higher than that calculated at the HF/6-31G(d,p) level. The data in Table 2 clearly reveal that, at the HF level of calculation, the use of split-valence basis sets and polarization functions lead to a decrease in the values of ΔE_T for the conformers of 2-MTHP. This trend is more pronounced when diffuse functions are incorporated into the basis sets.

Table 2. Comparison between the relative energies (kcal/mol) of the conformers of 2-methoxytetrahydropyran calculated by different ab initio methods

Method		Conformer					
		(+sc, +sc)	(+sc, ap)[e]	(+sc, −sc)	(ap, +sc)	(ap, ap)	(ap, −sc)
HF	3-21G[a]	0.00	—	—	6.73	—	3.70
	4-21G[b]	0.00	4.81	11.23	5.44	9.81	3.67
	6-31G(d)[b]	0.00	4.00	10.53	4.38	6.03	1.47
	6-31G(d,p)[c]	0.00	3.93	10.46	4.31	5.95	1.39
	6-31+G(d)[b]	0.00	3.82	10.10	4.05	5.58	1.08
	6-311++G(d)[b]	0.00	3.68	10.11	3.93	5.48	0.94
	cc-pVDZ[d]	0.00	4.70	—	—	—	—
MP2	6-31G(d)[b]	0.00	4.57	10.50	5.10	7.01	2.23
	6-311++G(d,p)[b]	0.00	3.56	9.96	3.66	5.24	0.65
GVB-PP	6-31G(d,p)[c]	0.00	3.95	10.55	4.36	5.98	1.52

[a] Ref. 14.
[b] Ref. 16.
[c] This work.
[d] Ref. 17.
[e] Except for the present calculations, the designation (+sc, ap) is correct because $\phi \geqslant 150°$.

The MP2 calculations, as already pointed out by Tvaroška and Carver,[16] seem not to provide a good description of the relative energy of the (ap, −sc) structure, because the values found at both MP2/6-31G(d) and MP2/6-311++G(d,p) levels are rather different from those obtained at the HF/6-31G(d) and 6-31G(d,p) levels (Table 2). The relative energies of the (ap, −sc) conformer obtained at the HF/6-31G(d)[16] and 6-31G(d,p) levels are indeed comparable to the gas-phase experimental value reported for 4,6-Me_2-2-MTHP.[38]

The potential curves for rotation about the exocyclic C1–O1 bond for both axial and equatorial forms of 2-MTHP were constructed at the HF/6-31G(d,p) and GVB-PP/6-31G(d,p) levels and are depicted in Figure 2. For each conformer of 2-MTHP, the HF and GVB-PP potential curves exhibit analogous profiles, leading to similarities in the geometry of the conformational minima and in the values and location of the internal rotation barriers.

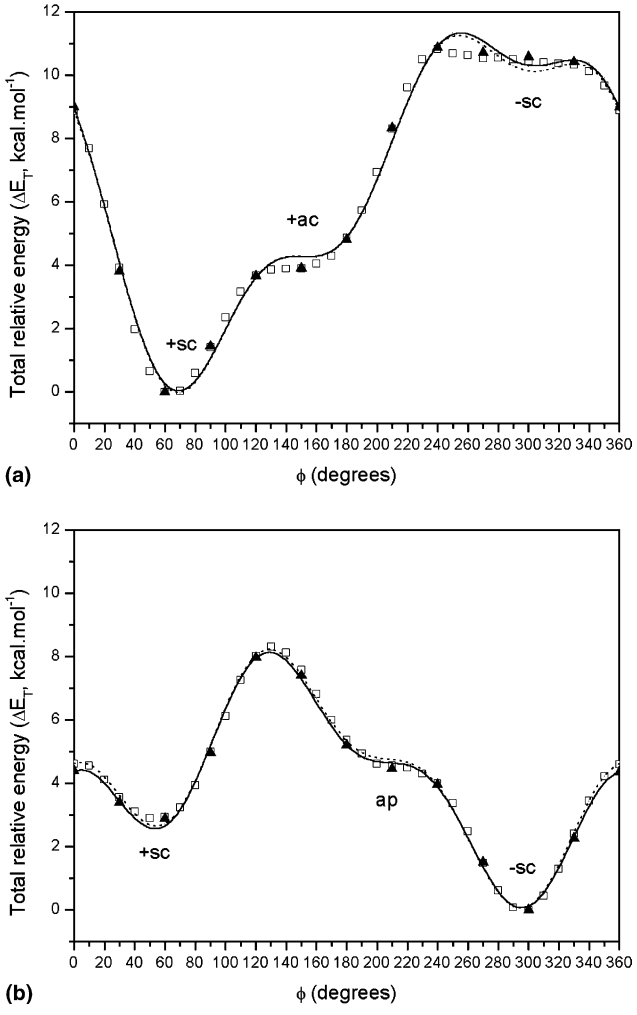

Figure 2. Potential curves for rotation about the C1–O1 bond for the axial (a) and equatorial (b) forms of 2-methoxytetrahydropyran calculated at both HF/6-31G(d,p) (□; dotted line) and GVB-PP/6-31G(d,p) (▲; solid line) levels.

Both HF and GVB-PP potential curves for the axial form (Fig. 2a) show a global minimum in the (+sc) region. This minimum is assigned to the (+sc, +sc) conformer. A local minimum appears in the (−sc) region and is assigned to the (+sc, −sc) conformer. Only a plateau can be observed in the (+ac) region of the axial potential curves; however, we could optimize the HF and GVB-PP geometries of the (+sc, +ac) conformer without any geometric constraints. It is important to mention that at the MP2/6-31G(d) level of calculation a conformational minimum was also found in the (+ac) region of the axial curve.[16] Two rotational barriers separate the (+sc, +sc) and (+sc, −sc) conformers. The barrier at $\phi = 250°$ is approximately of 11 kcal/mol, and the rotational barrier at $\phi = 330°$ is worth about 10 kcal/mol.

In the potential curves for the equatorial form of 2-MTHP (Fig. 2b), a global minimum is found in the −sc region and refers to the (ap, −sc) conformer. The next most stable conformer is the (ap, +sc) one. There is no local minimum in the (ap) region of both HF and GVB-PP equatorial potential curves. Thus, to optimize the geometry of the (ap, ap) conformer, we had to fix the value of ϕ at 210° during the optimization processes. This value was chosen inasmuch as it lies at the center of the plateau covering the interval from 200° to 220°. No rotational barrier separates the (ap, ap) conformer from the (ap, −sc) one; however, there are two rotational barriers separating the (ap, −sc) and (ap, +sc) conformers. The barrier at $\phi = 0°$ is approximately equal to 4 kcal/mol, whereas the barrier at $\phi = 130°$ is worth about 8 kcal/mol.

3.2. Geometric parameters

Selected geometric parameters calculated for the axial and equatorial conformers of 2-MTHP are listed in Tables 3 and 4. Indeed, the most important geometric parameters are those associated to the C5–O5–C1–O1–Ci fragment, because they differ significantly among the conformers. Tables 3 and 4 show that the optimized values of the torsion angles θ and ϕ exhibit negligible variations with the level of calculation. The structures optimized at the GVB-PP/6-31G(d,p) level are presented in Figure 3.

For the (+sc, +sc) conformer, the calculated values of θ and ϕ are very close to the expected ones, shown in Figure 1. The same occurs for the equatorial (ap, +sc) and (ap, −sc) conformers. Regarding the (+sc, +ac) conformer, the HF and GVB-PP values obtained for θ are very similar to the expected one; however, the optimized values of ϕ are about 40° lower than the one indicated in Figure 1. This result forced us to change the designation of ϕ from (ap) to (+ac), according to

Table 3. Selected geometric parameters for the axial conformers of 2-methoxytetrahydropyran calculated at the HF/6-31G(d,p) and GVB-PP/6-31G(d,p) levels[a]

	HF/6-31G(d,p)			GVB-PP/6-31G(d,p)		
	(+sc, +sc)	(+sc, +ac)	(+sc, −sc)	(+sc, +sc)	(+sc, +ac)	(+sc, −sc)
Bond lengths						
C5–O5	1.411	1.411	1.410	1.437	1.437	1.437
O5–C1	1.393	1.383	1.393	1.416	1.407	1.416
C1–O1	1.388	1.398	1.396	1.410	1.422	1.420
O1–Ci	1.399	1.394	1.395	1.427	1.421	1.421
C1–H	1.087	1.086	1.081	1.104	1.103	1.099
C1–C2	1.522	1.527	1.536	1.541	1.545	1.555
Bond angles						
Ci–O1–C1	115.17	116.10	120.85	113.96	114.61	119.45
O1–C1–O5	111.83	109.15	113.35	112.06	109.12	113.72
C1–O5–C5	115.47	115.52	121.30	114.40	114.38	120.02
O5–C5–C4	111.35	111.10	112.77	111.31	111.03	112.83
O5–C1–H	111.35	111.10	112.77	111.31	111.03	112.83
O1–C1–H	109.71	109.60	102.84	109.74	109.73	102.43
Dihedral angles						
ϕ	64.59	140.92	−47.46	64.10	141.24	−47.15
θ	64.64	64.22	94.14	63.88	63.17	94.18
C2–C1–O1–Ci	−173.14	−97.12	85.02	−172.38	−96.07	85.06

[a] Bond lengths are given in angstroms and angles in degrees.

Table 4. Selected geometric parameters for the equatorial conformers of 2-methoxytetrahydropyran calculated at the HF/6-31G(d,p) and GVB-PP/6-31G(d,p) levels[a]

	HF/6-31G(d,p)			GVB-PP/6-31G(d,p)		
	(ap, +sc)	(ap, ap)	(ap, −sc)	(ap, +sc)	(ap, ap)	(ap, −sc)
Bond lengths						
C5–O5	1.404	1.403	1.403	1.430	1.430	1.430
O5–C1	1.397	1.388	1.398	1.421	1.414	1.422
C1–O1	1.378	1.395	1.372	1.402	1.408	1.396
O1–Ci	1.403	1.395	1.401	1.430	1.422	1.428
C1–H	1.089	1.096	1.096	1.106	1.111	1.112
C1–C2	1.526	1.525	1.518	1.544	1.543	1.537
Bond angles						
Ci–O1–C1	118.24	116.13	115.71	117.00	114.53	114.49
O1–C1–O5	109.13	105.49	108.90	109.03	104.94	108.71
C1–O5–C5	114.27	114.27	114.06	113.04	112.97	112.85
O5–C5–C4	111.27	111.35	110.92	111.23	111.27	110.84
O5–C1–H	109.06	109.08	108.16	109.08	109.09	108.30
O1–C1–H	104.86	109.80	109.95	104.44	109.91	109.95
Dihedral angles						
ϕ	54.75	210.00	−63.08	54.64	210.00	−62.89
θ	172.57	178.90	179.28	171.62	177.56	178.89
C2–C1–O1–Ci	−68.46	91.53	176.95	−69.41	90.19	176.56

[a] Bond lengths are given in angstroms and angles in degrees.

Klyne–Prelog's rule. As mentioned before, in the HF and GVB-PP potential curves for the equatorial form of 2-MTHP (Fig. 2b), the absence of a local minimum at $\phi = 180°$ is evident. On the other hand, a plateau can be clearly observed in the range from 200° to 220°. Hence, we set ϕ to 210° to obtain the structure of the equatorial (ap, ap) conformer in both HF and GVB-PP calculations. Nevertheless, the optimized values of θ for (ap, ap) are closer to the expected one (Fig. 1). For the axial (+sc, −sc) conformer, neither the values of θ nor the values of ϕ are closer to the expected ones (Fig. 1). Due to steric repulsions between the aglycone methyl group and the axial hydrogen atoms bound to the C3 and C5 atoms, the HF and GVB-PP values of θ and ϕ for (+sc, −sc) were strongly affected, leading to a considerable distortion of the heterocyclic ring (Fig. 3). As a consequence (+sc, −sc) is the less stable conformer of 2-MTHP (Table 1).

The bond distances of the C5–O5–C1–O1–Ci moiety calculated in this work are plotted against the order of

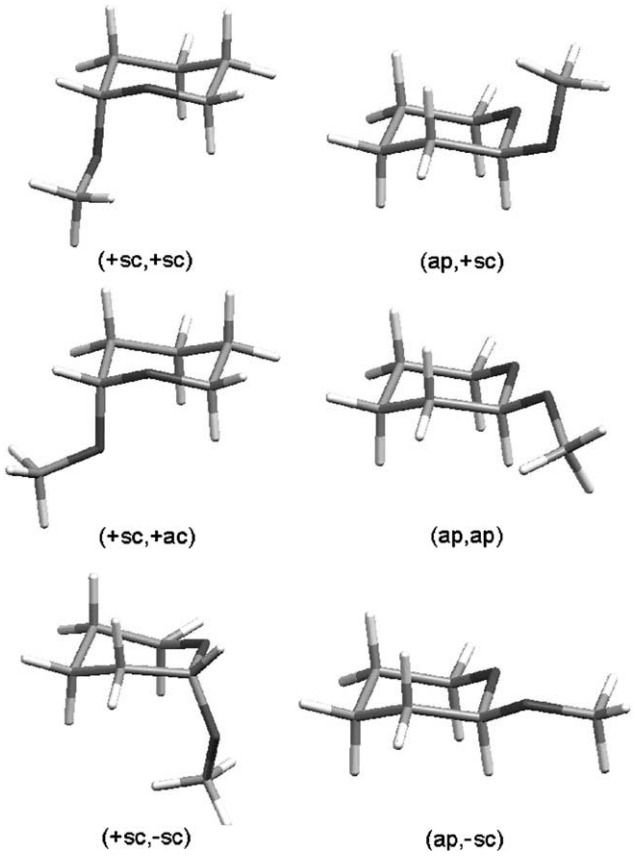

Figure 3. The structures of the axial and equatorial conformers of 2-methoxytetrahyropyran optimized at the GVB-PP/6-31G(d,p) level.

stability of the conformers of 2-MTHP in Figure 4. As a general result, for a given chemical bond, the GVB-PP bond length is longer than the corresponding HF one. Furthermore, the plots in Figure 4 show that the HF conformational changes in bond lengths are well reproduced at the GVB-PP level of calculation. A different pattern is observed for the (ap, ap) conformer when both descriptions are compared. For this last conformer, the O5–C1 bond is the shortest one at the HF level, while at the GVB-PP level the C1–O1 becomes the shortest one. The GVB-PP bond angles are, in general, smaller than the ones obtained at the HF level (Tables 3 and 4, Fig. 5).

The manifestation of both anomeric and exo-anomeric effects, as described in the literature,[5] seems to result from a combination of two electronic factors. The first and the less studied factor concerns the electrostatic repulsion between coplanar isolated pairs of electrons on the O5 and O1 atoms (namely the rabbit-ear effect), which based on the present knowledge, can only reasonably account for the order of stability of the conformers. The second and more generally accredited factor, the hyperconjugation effect, is supported by results of NBO analysis and is used to explain not only the order of stability of the conformers, but also some geometric changes, which are indeed observed in many crystal structures of carbohydrates. As we have highlighted in the 'Introduction' section, the anomeric effect is generally viewed as a result of the delocalization of a coplanar lone pair of the O5 atom to the antibonding σ^*_{C1-O1} orbital. Such hyperconjugative charge-transfer interaction is assumed to be responsible for the O5–C1 bond shortening and the C1–O1 bond lengthening. In the case of the exo-anomeric effect, attributed to the $n_{O1} \rightarrow \sigma^*_{C1-O5}$ delocalization effect, it is expected that the preference for the (+sc) or (−sc) orientations around glycosidic C1–O1 bonds is followed by the C1–O1 bond shortening and the increase of the O5–C1 bond length. In fact, none of the MO calculations on carbohydrates or model

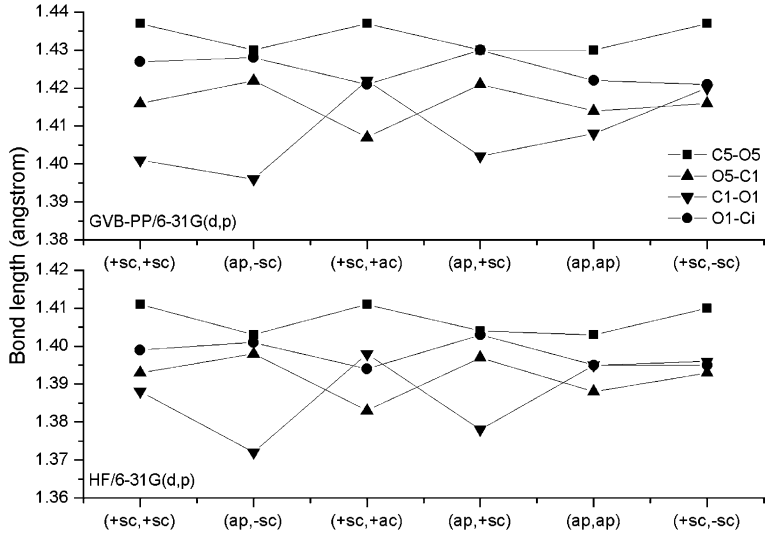

Figure 4. Bond distances of the C5–O5–C1–O1–Ci fragment for the six conformers of 2-methoxytetrahydropyran calculated at both HF/6-31G(d,p) and GVB-PP/6-31G(d,p) levels.

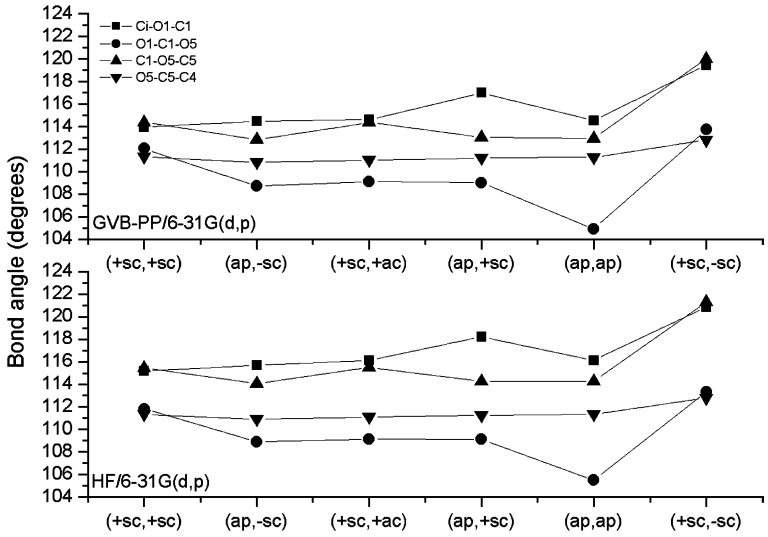

Figure 5. Comparison between some bond angles of the C5–O5–C1–O1–Ci fragment calculated at both HF/6-31G(d,p) and GVB-PP/6-31G(d,p) levels for the six conformers of 2-methoxytetrahydropyran.

compounds has explicitly included any couplings between these bonding and antibonding orbitals. However, the geometric data extracted from those calculations have been widely employed to justify the presence of the hyperconjugative interactions. From a quantitative point of view, the role played by the hyperconjugation effects (if any) in defining the geometry and relative stability of the conformers of 2-MTHP is not evident from our HF/6-31G(d,p) calculations.

A clean way of searching for the actual contributions (in the MO context) of hyperconjugative interactions would be to construct a multi-configurational (MCSCF) wave function including the appropriate configurations and variationally determine their weights for the energy of the conformers. Because HF is a single-configuration wave function, it does not explicitly contain contributions of the type $n_{O5} \rightarrow \sigma^*_{C1-O1}$ and $n_{O1} \rightarrow \sigma^*_{C1-O5}$. These mixings are introduced a posteriori in the process of transforming the optimized HF orbitals into the NBOs. However, whereas the original HF orbitals are obtained according to a given prescription, that is, minimization of the energy functional, the NBOs are obtained through a series of transformations that bear no relation to the energy-minimization criterion, which originated the HF orbitals being transformed. Therefore, any contributions from such mixings are being determined by criteria (maximum occupancy, etc.) other than the ones used to obtain the optimum HF orbitals. Besides that, as mentioned previously, because the HF (or MO) orbitals are not uniquely defined within a given basis set, the NBOs are also not uniquely defined.

The GVB-PP approach does not include any couplings between lone pairs and σ^* orbitals, that is, this method describes orbitals strictly localized on atomic centers. Because the HF approach deals with delocalized orbitals, it is surprising to verify that the HF and GVB-PP optimized structures of 2-MTHP present the same order of stability (Table 1), as well as the same conformational trends in bond lengths and angles (Figs. 4 and 5). Therefore, due to all the reasons aforementioned, we believe that the use of the electronic hyperconjugation concept to explain the origin of the anomeric and exo-anomeric effects ought to be reconsidered.

3.3. The GVB-PP description of the chemical bond in the C5–O5–C1–O1–Ci moiety: the nature of the anomeric and exo-anomeric effects

The quantum-mechanical translation of the classical concept of the covalent bond can only be achieved when an Independent Particle Model (IPM) is used to describe the N electrons of the molecule and when the proper permutation symmetry of the electronic wave function is retained.[45] These requirements are satisfied by the GVB[42] and SCVB (spin coupled valence bond)[46] wave functions—based on the valence bond (VB) theory. VB-based methods are capable of providing *uniquely defined* (within a given basis set) one-electron states, which are required to properly define a chemical structure and the chemical bonds. On the other hand, molecular orbitals are not uniquely defined and are generally delocalized over the entire molecule.

The use of molecular orbitals in chemical bonding discussions usually relies on some sort of a posteriori procedure (which always has some degree of arbitrariness) to localize the orbitals, that is, to make the MO wave function 'look like' a valence bond. Therefore, any attempts to investigate the nature of the chemical phenomena using the concepts of chemical structure

and chemical bond should be made through the use of GVB or SCVB wave functions, as discussed in great detail elsewhere.[45]

In the present study, we employ the GVB method to interpret the origin of the order of stability and conformational changes in geometric parameters of the conformers of 2-MTHP using the concepts of chemical bond and chemical structure. Our choice can be more clearly justified as follows. The GVB approach (as the old VB approach) represents the quantum-mechanical translation of the Lewis structures, and the best (optimized) orbitals (atomic orbitals) describing the chemical bonds emerge *directly* from the self-consistent calculations. The NBO analysis, which is widely used to interpret the origin of the anomeric and exo-anomeric effects, starts from a wave function (HF) that describes the molecular structure by delocalized orbitals and *indirectly* tries to recover, through a series of transformations (including the mixing of the occupied and unoccupied orbitals) something that would be equivalent to the Lewis structures. In this case, the difference in energy between the optimized HF structure and the NBO-Lewis structure (less stable) is interpreted as being due to electronic delocalization (such as hyperconjugation) effects. It is interesting to observe that the NBO analysis is just an attempt to mimic, from HF-type calculations, the results that can be clearly, elegantly, self-consistently, and uniquely obtained from VB-type calculations.

Of all the possible spin-coupling schemes involved in the formation of chemical bonds in molecules, the pairing between electrons of adjacent atomic-centered non-orthogonal singly occupied orbitals in general plays the most important role. The GVB wave function in its perfect pairing (PP) approach deals exactly with this type of spin-coupling scheme.[42] Owing to this, we decided to use the self-consistently obtained GVB-PP wave functions to study not only the nature of the chemical bond in both axial and equatorial acetal moieties of 2-MTHP, but also the origin of the anomeric and exo-anomeric effects.

The optimum non-orthogonal GVB orbitals for a group of atoms of the (+sc, +sc) conformer, including those of the acetal fragment, are illustrated in Figure 6. For the sake of clarity, in Figure 6 the two GVB orbitals that form a given chemical bond are shown in the same row (in separate columns) along with the overlap integral, S_{A-B}, associated to the bond. In the GVB-PP method, each chemical bond is represented in terms of a pair of GVB orbitals localized in the internuclear region. Because each electron is described by one GVB orbital, each singlet-coupled pair i of electrons is described by two non-orthogonal GVB orbitals, ϕ_A^i and ϕ_B^i (symmetric with respect to the bond axis), centered on the atoms A and B, respectively. Similarly, each oxygen lone pair is described by two GVB orbitals

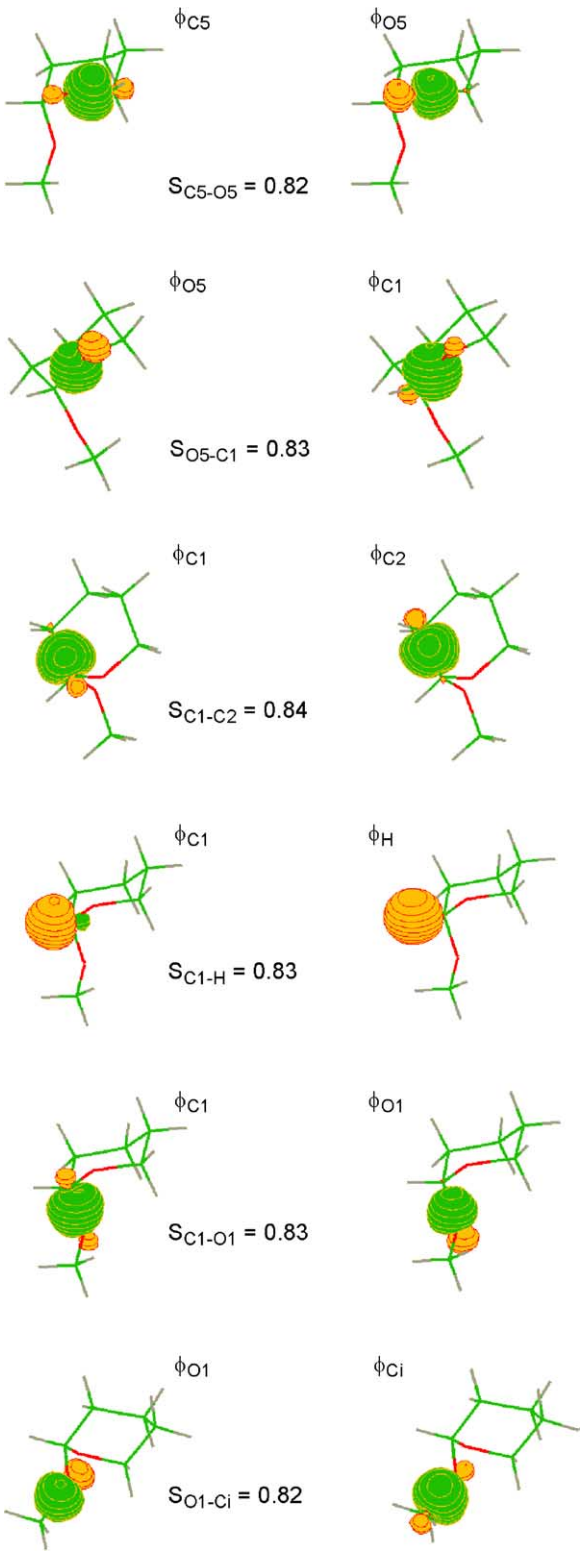

Figure 6. Non-orthogonal GVB orbitals optimized for a group of atoms of the (+sc, +sc) conformer of 2-methoxytetrahydropyran. Green and yellow contours indicate positive and negative amplitudes, respectively, with spacing of 0.1 a.u. between the contours.

oriented in the same direction, one being more diffuse than the other. Figure 7 shows the optimum GVB orbitals

describing the lone pairs on the O5 and O1 atoms of the (+sc, +sc) conformer. In this figure, the pair of non-orthogonal GVB orbitals associated with a given lone pair is illustrated in the same row, in separate columns. Regardless of the conformer, the value of the overlap integral for the GVB orbitals describing each oxygen lone pair is equal to 0.89.

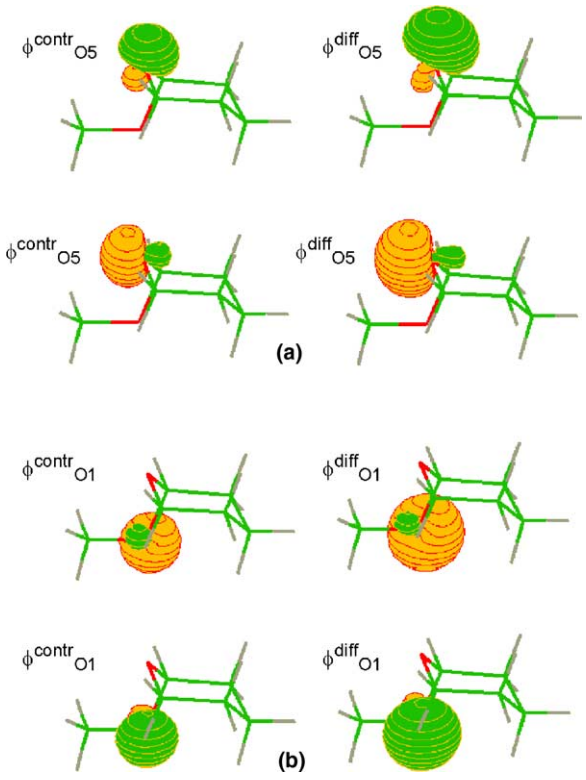

Figure 7. Orientation of the optimum GVB orbitals associated with the lone pairs on the O5 (a) and O1 (b) atoms of the (+sc, +sc) conformer (contr and diff stand for contracted and diffuse, respectively). Green and yellow contours indicate positive and negative amplitudes, respectively, with spacing of 0.1 a.u. between the contours.

In contrast to the classical VB model, in the GVB approach no previous hybridization is imposed to the atomic orbitals. Moreover, the orbitals are allowed to acquire their best shapes, polarizing onto adjacent centers when needed but still preserving their atomic-like nature. Thus, the optimum non-orthogonal GVB orbitals will not necessarily exhibit exact sp, sp^2, sp^3, etc., characters but the most appropriate combination for a particular bond and chemical environment. Thus, to distinguish between the GVB orbitals and the standard hybrid orbitals used in the old VB theory, one refers the self-consistently obtained non-orthogonal GVB orbitals with mixed character as 'lobe' orbitals.

To investigate the nature of the chemical bond in the axial and equatorial acetal fragments of 2-MTHP, we have chosen the (+sc, +sc) and (ap, −sc) conformers because they are the most abundant ones and also because the anomeric and exo-anomeric effects are pronounced in these conformers. Table 5 shows the composition (in terms of the percentage of s, p, and d character) of some GVB orbitals optimized for both (+sc, +sc) and (ap, −sc) conformers along with the overlap integrals S_{A-B}. In Table 5 one also observes that the character of each 'lobe' GVB orbital relies on the type of the bond and on the conformer. Possibly, the differences in character observed for the GVB orbitals describing the chemical bonds in the acetal fragments respond for the observed differences in bond lengths and angles.

In Section 3.2 we have questioned the usage of electronic hyperconjugation interactions to account for the structural trends observed in acetal fragments. Thus, in view of our interest in using the GVB-PP results to explain the conformational changes in bond lengths of 2-MTHP, we have tried to correlate the %s character on the carbon atoms with the bond distances of the acetal

Table 5. Percentage of s, p, and d character of some optimized GVB orbitals of the (+sc, +sc) and (ap, −sc) conformers and some overlap integrals

Bond	(+sc, +sc)						(ap, −sc)					
	Bond length[a]		%s	%p	%d	S_{A-B}	Bond length		%s	%p	%d	S_{A-B}
C5–O5	1.437	ϕ_{C5}	19.7	78.8	1.5	0.821	1.430	ϕ_{C5}	20.3	78.2	1.5	0.822
		ϕ_{O5}	15.3	84.3	0.4			ϕ_{O5}	15.3	84.3	0.4	
O5–C1	1.416	ϕ_{O5}	16.2	83.3	0.5	0.830	1.422	ϕ_{O5}	15.3	84.3	0.4	0.827
		ϕ_{C1}	22.0	75.6	2.4			ϕ_{C1}	20.6	77.1	2.3	
C1–O1	1.410	ϕ_{C1}	22.1	75.8	2.1	0.831	1.396	ϕ_{C1}	23.6	74.8	1.6	0.831
		ϕ_{O1}	15.9	83.6	0.5			ϕ_{O1}	16.4	83.2	0.4	
O1–Ci	1.427	ϕ_{O1}	15.2	84.4	0.4	0.822	1.428	ϕ_{O1}	15.4	84.2	0.4	0.822
		ϕ_{Ci}	20.6	77.6	1.8			ϕ_{Ci}	20.4	77.5	2.1	
C1–C2	1.541	ϕ_{C1}	33.4	65.5	1.1	0.841	1.537	ϕ_{C1}	32.5	66.2	1.3	0.842
		ϕ_{C2}	27.4	70.8	1.8			ϕ_{C2}	28.2	70.8	1.0	
C1–H	1.104	ϕ_{C1}	32.3	66.7	1.0	0.832	1.112	ϕ_{C1}	32.0	66.4	1.6	0.832
		ϕ_{H}	100.0	0.0	—			ϕ_{H}	100.0	0.0	—	
Lone pairs[b]		ϕ_{contr}	38–39	60–61	~0.5	0.89		ϕ_{contr}	38–39	60–61	~0.5	0.89
		ϕ_{diff}	32–33	66–67	~0.9			ϕ_{diff}	32–33	66–67	~0.9	

[a] Bond lengths are given in angstroms.
[b] Contr and diff stand for contracted and diffuse, respectively.

moieties of both (+sc, +sc) and (ap, −sc) conformers. In Figure 8, the %s character of each GVB orbital on the C atoms (C1, C5, or Ci) is plotted as a function of the C5–O5, O5–C1, C1–O1, and O1–Ci bond distances for both (+sc, +sc) (Fig. 8a) and (ap, −sc) (Fig. 8b) conformers. Additionally, in Figure 8 the sum of the percentages of s character of both carbon- and oxygen-centered orbitals are plotted against the C–O bond distances. There appears to be a linear correlation for both conformers, implying that the higher the %s character on the C orbital (or on the sum C + O) the shorter the bond length at the acetal fragment. In other words, not only the %s character on the C orbitals, but also the sum of the s characters of the C- and O-centered orbitals linearly correlates to the bond distances of the acetal moieties in both (+sc, +sc) and (ap, −sc) conformers. This is in conformity to what is observed for the C–H bond lengths in hydrocarbons, for example. As the percentage of s character of the carbon hybrid orbitals increases

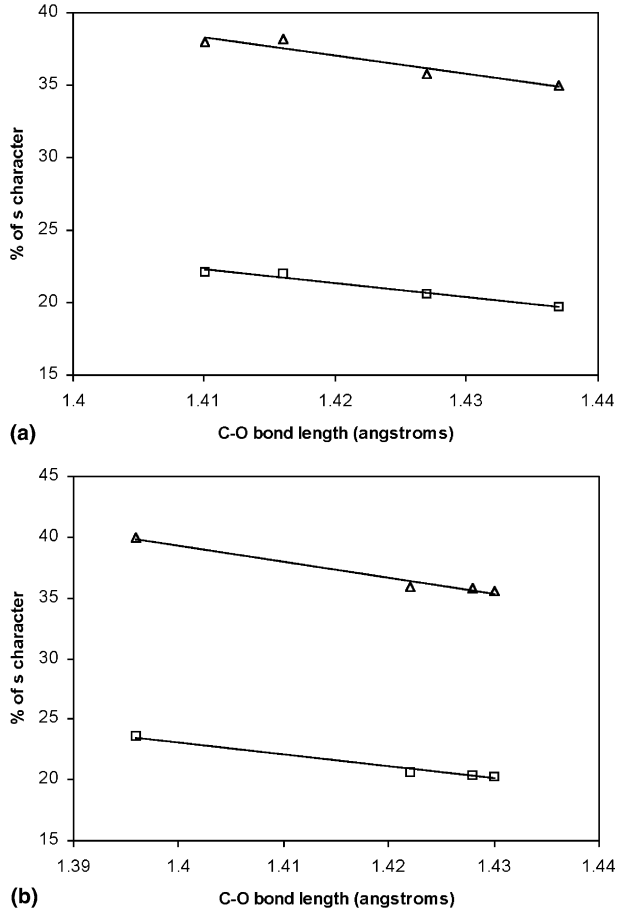

Figure 8. Correlation between the percentage of s character of the GVB orbitals on the C1, C5, or Ci (square) atoms and the C5–O5, O5–C1, C1–O1, and O1–Ci bond lengths for the (+sc, +sc) (a) and (ap, −sc) (b) conformers. A correlation between the sum of the percentages of s character on the C and O (triangle) GVB orbitals and the same bond distances is also shown.

(from sp^3 to sp^2 and sp), the bond lengths shorten, reflecting the better overlap of the bonding orbitals. Therefore, the changes in bond lengths normally attributed to the anomeric and exo-anomeric effects can be simply understood as resulting from a change in the character of the bonding orbitals, without having to rely on hyperconjugation effects.

Based on the GVB-PP results, the order of stability of the conformers of 2-MTHP can be explained by the analysis of steric and lone-pair repulsions. Figure 9 shows the more diffuse GVB orbitals describing the lone pairs on the O5 and O1 atoms of all conformers of 2-MTHP. The most stable conformer of 2-MTHP (+sc, +sc), does not present any steric repulsion between the aglycone methyl group and axial (or equatorial) hydrogen atoms as well as any repulsive interaction between coplanar lone pairs (known as rabbit-ear interaction[5]). The (ap, −sc) is the second most stable conformer of 2-MTHP probably because it only exhibits one rabbit-ear interaction. The (+sc, +ac) conformer presents one rabbit-ear interaction, and its structure leads to a steric repulsion between the aglycone methyl group and the H atom attached to C1. For the (ap, +sc) conformer, in addition to one rabbit-ear interaction, the steric repulsion between the aglycone methyl group and the axial H atom bound to C2 must be taken into account. The energy difference between the (+sc, +ac) and (ap, +sc) conformers is 0.4 kcal/mol (in favor of the former) at the GVB-PP level (Table 1). Due to this very small energy difference between the (+sc, +ac) and (ap, +sc) conformers, it is difficult to predict the most stable one from a qualitative analysis of the repulsive interactions. In the case of the (+sc, −sc) conformer, one rabbit-ear interaction and the steric repulsion between the methyl group and the axial hydrogen atoms on the C3 and C5 lead to the less stable conformation of 2-MTHP. The equatorial (ap, ap) conformer is the only one to exhibit two rabbit-ear interactions. This is probably the reason by which the (ap, ap) conformer is the second less stable conformer of 2-MTHP.

Before concluding this section it is worth briefly reviewing some previous discussions about the origin of the anomeric and exo-anomeric effects. The anomeric effect was first interpreted by Edward[6] in terms of the electrostatic repulsion between the exocyclic C–O bond dipole and the resultant dipole on the endocyclic oxygen atom due to the lone pairs. This explanation failed to describe the order of stability of conformers about the exocyclic C–O bond, that is, the exo-anomeric effect. Due to this, Eliel,[37] Lemieux,[11] and others[12] tried to explain the order of stability of the different conformations about the glycosidic C1–O1 bond by proposing the rabbit-ear effect. Insofar as this proposal was based solely on qualitative grounds, the actual shapes, composition and orientation of the oxygen lone pairs were not discussed in

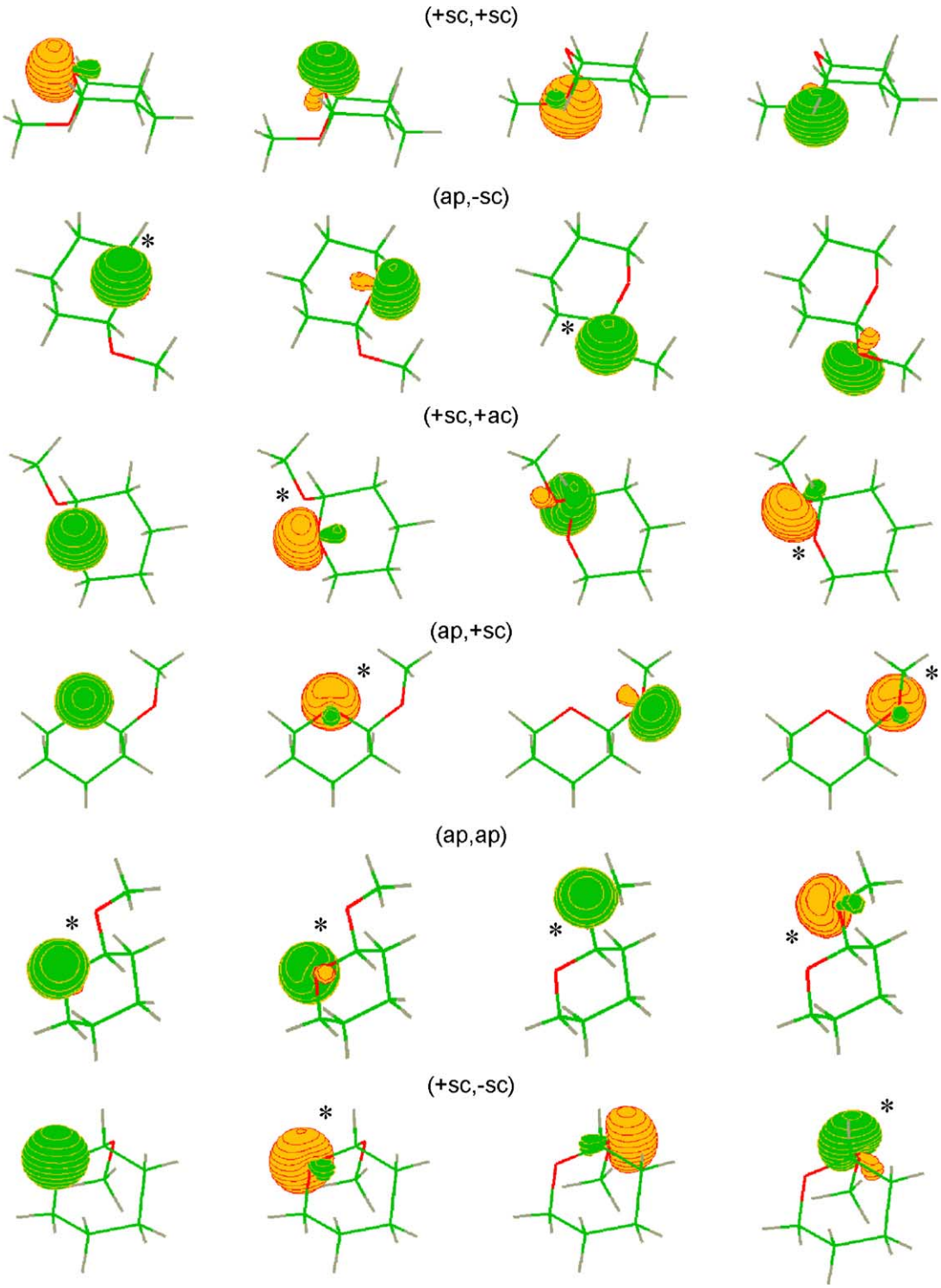

Figure 9. Orientation of the more diffuse GVB orbitals describing the lone pairs on the O5 and O1 atoms of all conformers of 2-methoxytetrahydropyran. Asterisks indicate the GVB orbitals involved in the rabbit-ear interaction. Green and yellow contours indicate positive and negative amplitudes, respectively, with spacing of 0.1 a.u. between the contours.

detail. Thus, the rabbit-ear effect reasonably explained the order of stability of the conformers but failed to explain conformational changes in geometric parameters. In the late 1970s, Jeffery et al.[13] used the MO theory (HF calculations) to study the dimethoxymethane (DMM) molecule (an acyclic model for the acetal moiety) and observed that their computational results reproduced not only the order of stability of the

conformers in accordance with the experimental data, but also the conformational changes in bond lengths and angles that had been previously verified by X-ray and neutron diffraction on pyranosides. The results of the HF calculations on DMM and on the other model compounds (such as 2-MTHP) were then interpreted in terms of hyperconjugative charge-transfer interactions, and NBO calculations have been used in support of that. Owing to the rapid acceptance of the 'delocalized' interpretation of the anomeric and exo-anomeric effects, the rabbit-ear approach was abandoned at an early stage of its development. In this paper, a more quantitative description of the rabbit-ear effect was obtained (from the actual shapes and orientation of the O5 and O1 lone pairs), and this effect together with the steric repulsions between the aglycone methyl group and hydrogen atoms are evoked to explain the order of stability of the conformers of 2-MTHP in light of the GVB description. In doing so, the hyperconjugation concept was left aside, and we successfully correlated the %s character on the C atoms (and on the sum C + O) with the conformational changes in bond lengths in the axial and equatorial acetal moieties of 2-MTHP.

4. Conclusions

An ab initio study on the six conformers of 2-MTHP has been carried out at the HF/6-31G(d,p) and GVB-PP/6-31G(d,p) levels of calculation. At both levels, the order of stability of the conformers is the same, the axial (+sc, +sc) conformer being the most stable one, followed by the equatorial (ap, −sc) conformer. Moreover, the HF and GVB-PP potential curves for rotation about the axial and equatorial C1–O1 bonds of 2-MTHP exhibit analogous profiles, reflecting the similarities in the values of ϕ and in the position and values of the internal rotation barriers. Plots of the bond lengths and angles of the acetal moieties of 2-MTHP against the order of stability of the conformers show not only that there is no correlation between the order of stability and the values of these geometric parameters, but also that the HF conformational changes in bond lengths and angles are well reproduced in the GVB-PP calculations. As the GVB-PP approach does not include any couplings between lone pairs and σ^* orbitals, these results imply that the use of the electronic hyperconjugation concept to account for the origin of the anomeric and exo-anomeric effects may not be appropriate.

The nature of the chemical bond in the axial and equatorial acetal fragments of 2-MTHP has been discussed in terms of optimum non-orthogonal GVB orbitals of the (+sc, +sc) and (ap, −sc) conformers. Thus, it was possible to linearly correlate the %s character on the C atoms (and on the sum C + O) with the C5–O5, O5–C1, C1–O1, and O1–Ci bond distances. We propose that the higher the %s character the lower the value of the C–O bond length at the acetal moieties, in accordance with what is observed in other classes of compounds.

In light of the GVB-PP description, the order of stability of the conformers of 2-MTHP could be interpreted in terms of the steric repulsions between the aglycone methyl group and axial (or equatorial) H atoms and also by the analysis of the actual shapes and orientation of the GVB-PP orbitals describing the oxygen (O5 and O1) lone pairs. This latter analysis allowed a more comprehensive study of the rabbit-ear effect, that is, of the repulsive interactions between coplanar lone pairs on the O5 and O1 atoms.

Acknowledgements

The authors thank FAPERJ and CNPq for financial support.

References

1. Voet, D.; Voet, J. G. *Biochemistry*, 2nd ed.; John Wiley & Sons: New York, 1995, Chapter 10.
2. Rao, V. S. R.; Qasba, P. K.; Baslaji, P. V.; Chandrasekaran, R. *Conformation of Carbohydrates*; Harwood Academic: Amsterdam, 1998.
3. Woods, R. J. In *Reviews in Computational Chemistry*; Lipkowitz, K. B., Boyd, D. B., Eds.; VCH: New York, 1996; Vol. 9, pp 129–165.
4. Tvaroška, I.; Carver, J. P. *J. Phys. Chem.* **1995**, *99*, 6234–6241.
5. Tvaroška, I.; Bleha, T. *Adv. Carbohydr. Chem. Biochem.* **1989**, *47*, 45–123.
6. Edward, J. T. *Chem. Ind. (London)* **1955**, 1102–1104.
7. Lemieux, R. U. In *Molecular Rearrangements*; de Mayo, P., Ed.; Interscience: New York, 1964; Vol. 2, pp 709–769.
8. Lemieux, R. U.; Koto, S. *Tetrahedron* **1974**, *30*, 1933–1944.
9. Kirby, A. T. *The Anomeric Effect and Related Stereoelectronic Effects at Oxygen*; Springer: Berlin, 1983.
10. Deslongchamps, P. *Stereoelectronic Effects in Organic Chemistry*; Pergamon Press: Oxford, 1983, Chapter 2.
11. Lemieux, R. U.; Pavia, A. A.; Martin, J. C.; Watanabe, K. A. *Can. J. Chem.* **1969**, *47*, 4427–4439.
12. de Hoog, A. J.; Buys, H. R.; Altona, C.; Havinga, E. *Tetrahedron* **1969**, *25*, 3365–3375.
13. Jeffery, G. A.; Pople, J. A.; Binkley, J. S.; Vishveshwara, S. *J. Am. Chem. Soc.* **1978**, *100*, 373–379.
14. Wiberg, K. B.; Murcko, M. A. *J. Am. Chem. Soc.* **1989**, *111*, 4821–4828.
15. Salzner, U.; Schleyer, P. v. R. *J. Org. Chem.* **1994**, *59*, 2138–2155.
16. Tvaroška, I.; Carver, J. P. *J. Phys. Chem.* **1994**, *98*, 9477–9485.
17. Cramer, C. J.; Truhlar, D. G.; French, A. D. *Carbohydr. Res.* **1997**, *298*, 1–14.
18. Tvaroška, I.; Carver, J. P. *Carbohydr. Res.* **1998**, *309*, 1–9.
19. Momany, F. A.; Willett, J. L. *J. Comput. Chem.* **2000**, *21*, 1204–1219.

20. Cortés, F.; Tenorio, J.; Collera, O.; Cuevas, G. *J. Org. Chem.* **2001**, *66*, 2918–2924.
21. Martinez, K.; Cortés, F.; Leal, I.; Reyna, V.; Quintana, D.; Antunez, S.; Cuevas, G. *Arkivoc* **2003**, 132–148.
22. da Silva, C. O.; Nascimento, M. A. C. *Theor. Chem. Acc.* **2004**, *112*, 342–348.
23. Favero, L. B.; Caminati, W.; Velino, B. *Phys. Chem. Chem. Phys.* **2003**, *5*, 4776–4779.
24. Moon, S.; Kwon, Y.; Lee, J.; Choo, J. *J. Phys. Chem. A* **2001**, *105*, 3221–3225.
25. French, A. D.; Kelterer, A.-M.; Johnson, G. P.; Dowd, M. K. *J. Mol. Struct.* **2000**, *556*, 303–313.
26. Abe, A. *J. Am. Chem. Soc.* **1976**, *98*, 6477–6480.
27. Tvaroška, I.; Kozar, T. *J. Am. Chem. Soc.* **1980**, *102*, 6929–6935.
28. Tvaroška, I.; Kozar, T. *Theor. Chim. Acta.* **1986**, *70*, 99–114.
29. Navio, P. F.; Molina, J. M. *J. Mol. Struct.* **1990**, *222*, 387–400.
30. Imberty, A.; Hardman, K. D.; Carver, J. P.; Pérez, S. *Glycobiology* **1991**, *1*, 631–642.
31. Senderowitz, H.; Still, W. C. *J. Org. Chem.* **1997**, *62*, 1427–1438.
32. Hwang, M.-J.; Ni, X.; Waldman, M.; Ewig, C. S.; Hagler, A. T. *Biopolymers* **1998**, *45*, 435–468.
33. Eklund, R.; Widmalm, G. *Carbohydr. Res.* **2003**, *338*, 393–398.
34. Lii, J.-H.; Chen, H.-K.; Durkin, K. A.; Allinger, N. L. *J. Comput. Chem.* **2003**, *24*, 1473–1489.
35. Anderson, C. B.; Sepp, D. T. *Tetrahedron* **1968**, *24*, 1707–1716.
36. Pierson, G. O.; Runquist, O. A. *J. Org. Chem.* **1968**, *33*, 2572–2574.
37. Eliel, E. L.; Giza, C. A. *J. Org. Chem.* **1968**, *33*, 3754–3758.
38. Wiberg, K. B.; Marquez, M. *J. Am. Chem. Soc.* **1994**, *116*, 2197–2198.
39. Booth, H.; Grindley, T. B.; Khendhair, K. A. *J. Chem. Soc., Chem. Commun.* **1982**, 1047–1048.
40. Booth, H.; Khendhair, K. A.; Readshaw, S. A. *Tetrahedron* **1987**, *43*, 4699–4723.
41. Booth, H.; Dixon, J. M.; Readshaw, S. A. *Tetrahedron* **1992**, *48*, 6151–6160.
42. (a) Hunt, W. J.; Hay, P. J.; Goddard, W. A., III. *J. Chem. Phys.* **1972**, *57*, 738–748; (b) Hay, P. J.; Hunt, W. J.; Goddard, W. A., III. *J. Am. Chem. Soc.* **1972**, *94*, 8293–8301; (c) Goddard, W. A., III; Dunning, T. H., Jr.; Hunt, W. J.; Hay, P. J. *Acc. Chem. Res.* **1973**, *6*, 368–376; (d) Goddard, W. A., III; Bobrowicz, F. W. In *Methods of Electronic Structure Theory*; Schaefer, H. F., III, Ed.; Plenum Press: New York, 1977; Vol. 3, Chapter 4.
43. Jaguar 3.5, Schrödinger, Inc., Portland, OR, 1998.
44. Polygraf v3.2.1, Molecular Simulations, Inc., San Diego, CA, 1992.
45. (a) Barbosa, A. G. H. Ph.D. Thesis, Universidade Federal do Rio de Janeiro, 2002; (b) Barbosa, A. G. H.; Nascimento, M. A. C. In *Valence Bond Theory*; Cooper, D. L., Ed.; Elsevier: Amsterdam, 2002, pp 117–143; (c) Nascimento, M. A. C.; Barbosa, A. G. H. In *Fundamental World of Quantum Chemistry: A Tribute to Per-Olov Löwdin*; Brandas, E. J., Kryachko, E. S., Eds.; Kluwer: Dordrecht, 2003; Vol. 1, p 371.
46. (a) Gerratt, J.; Cooper, D. L.; Karadakov, P. B.; Raimondi, M. *Chem. Soc. Rev.* **1997**, *26*, 87–100; (b) Cooper, D. L.; Gerratt, J.; Raimondi, M. *Chem. Rev.* **1991**, *91*, 929–964.